Supporting Information

Integrating MWCNTs-doped MXene with multi-spiral-channel architecture enables field effect transistor biosensor capable of ultrasensitive determination of methotrexate

Chunwen Lu[a], Ping Xu[b], Dahui Wang[b,*], Dong Fu[b,*]

[a]Department of Orthopedics, Changhai Hospital, Second Military Medical University, Shanghai, China

[b]Department of Pediatric Orthopedics, Children's Hospital of Fudan University, National Children's Medical Center, Shanghai, China.

*Correspondence: wangdahui@fudan.edu.cn; fudong@fudan.edu.cn;

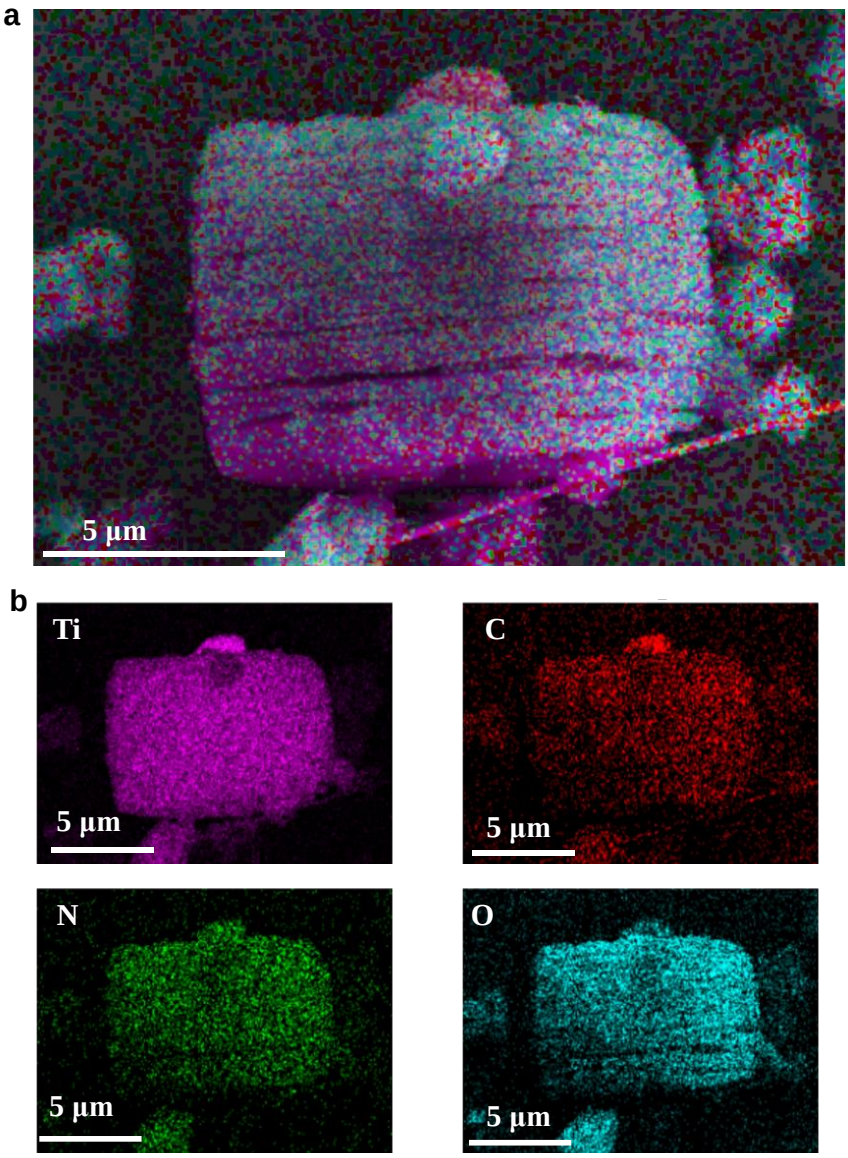

Fig. S1. a) Merged photography of SEM morphology for MXene with intercalation and delamination structures. Mapping analysis of MXene include b) Ti, C, N and O. The scale bars is 5 µm.

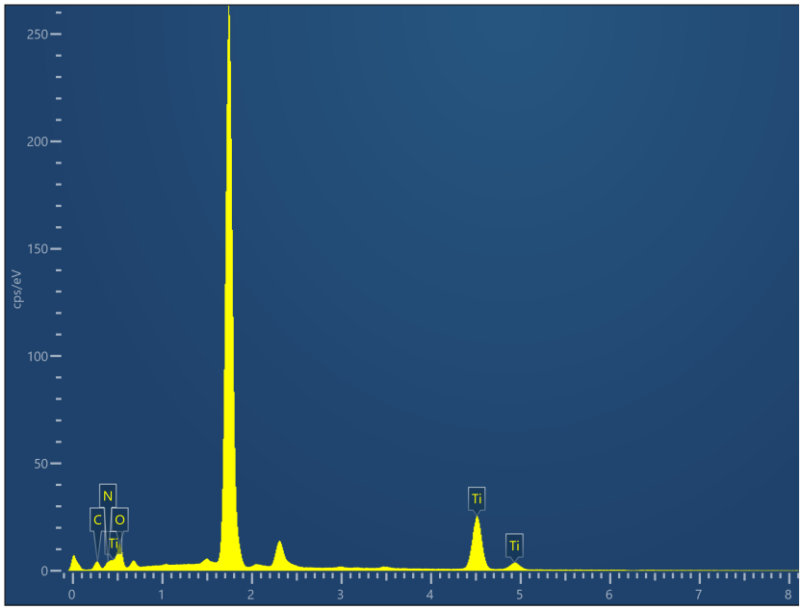

Fig. S2. The elemental analysis of MXene.

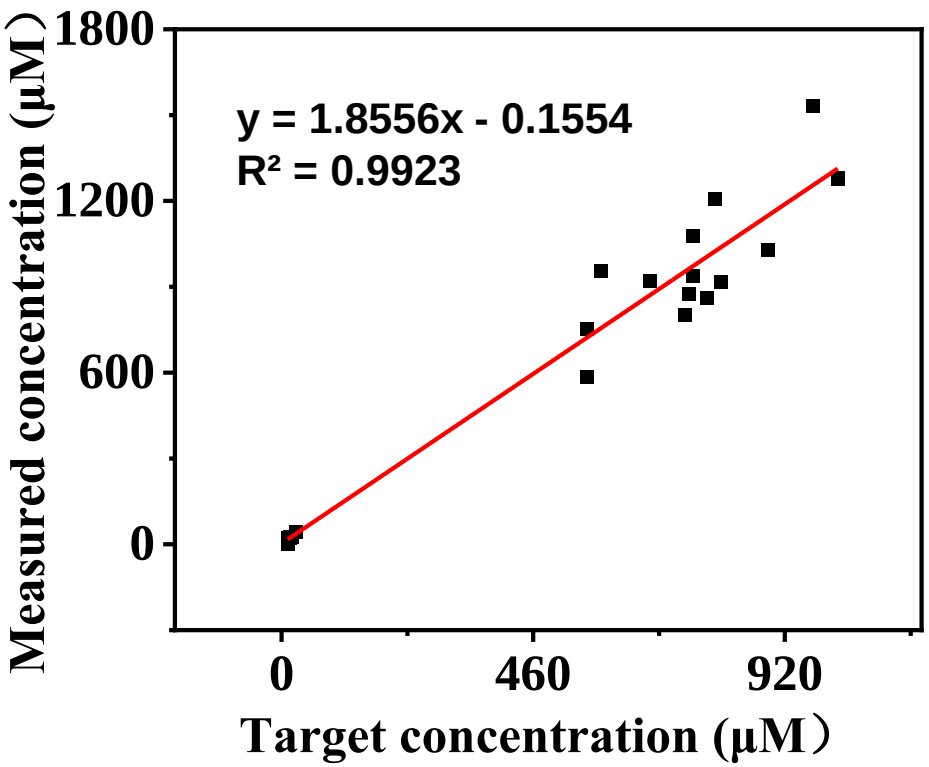

Fig. S3. The linear correlation of methotrexate's targeted concentration and measured concentration when methotrexate with the high concentration (＞10 μM).

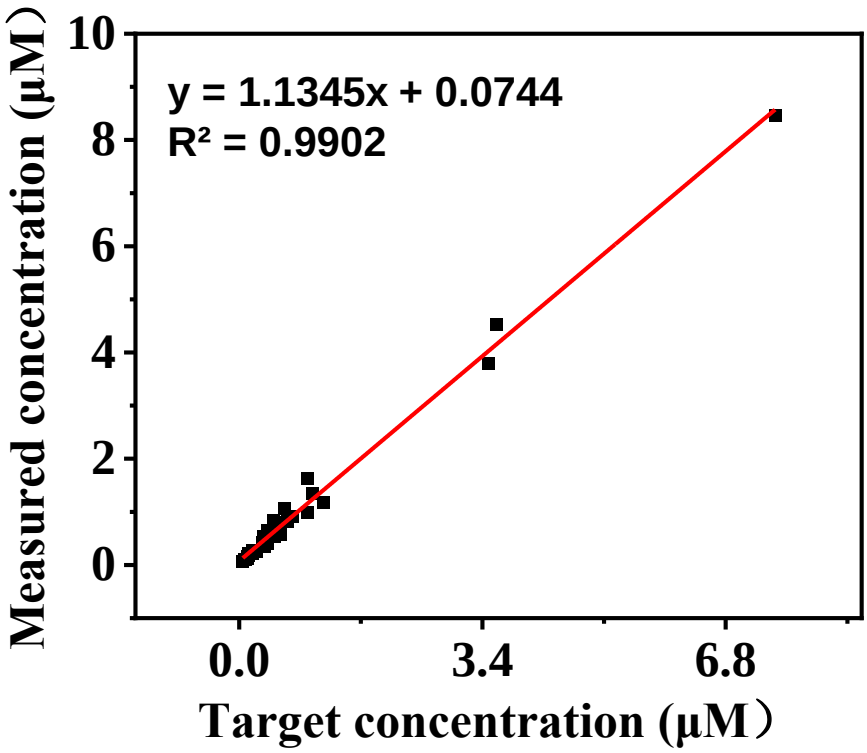

Fig. S4. The linear correlation of methotrexate's targeted concentration and measured concentration with methotrexate's concentrations rana between the 0-10 μM.

Table S1. The elemental analysis of MXene.

Elements	Type	Concentration	k ratio	Wt%	Wt% Sigma	Atomic percent
C	K	2.46	0.02457	8.89	0.23	17.30
N	K	0.00	0.00000	0.00	0.36	0.00
O	K	4.20	0.03681	39.35	0.40	57.46
Ti	K	27.16	0.27159	51.76	0.36	25.24
Total:				100.00		100.00

Table S2. The comparisons of biosensors for quantification of methotrexate.

Biosensor	**Linear detection**	**LOD**	**Reference**
N-doping hollow nanocarbon spheres/Glassy carbon electrode	0.05-14.0 μM	0.01 μM	(Li et al., 2021)
Acetylene black film/Glassy carbon electrode	0.005-3.0 μM	3.81 nM	(Deng et al., 2020)
Graphitic carbon nitride covered vanadium oxide nanocomposite/screen-printed carbon electrode	0.025-273.15 μM	13.26 nM	(Chen et al., 2019)
Au/Multi-walled carbon nanotubes-ZnO nanocomposite/ screen-printed electrode	0.02-1.00 μM	10 nM	(Wang et al., 2014)
MWCNTs/MXene-based FETs biosensor	0.001-100 μM	0.352 nM	This work

Table S3. The clinical information of 65 biosamples

Number of biosamples	Clinical targeted concentration of methotrexate (μmol/L)	The strategy of targeted concentration	The device	Measured concentration of methotrexate by MMSFETs (μmol/L)
1	0.05	Immunoluminescence	Abbott ARCHITECT I1000	0.089
2	0.07	Immunoluminescence	Abbott ARCHITECT I1000	0.117
3	0.09	Immunoluminescence	Abbott ARCHITECT I1000	0.097
4	0.11	Immunoluminescence	Abbott ARCHITECT I1000	0.203
5	0.11	Immunoluminescence	Abbott ARCHITECT I1000	0.139
6	0.11	Immunoluminescence	Abbott ARCHITECT I1000	0.128
7	0.13	Immunoluminescence	Abbott ARCHITECT I1000	0.250
8	0.13	Immunoluminescence	Abbott ARCHITECT I1000	0.153
9	0.13	Immunoluminescence	Abbott ARCHITECT I1000	0.164
10	0.18	Immunoluminescence	Abbott ARCHITECT I1000	0.257
11	0.18	Immunoluminescence	Abbott ARCHITECT I1000	0.275
12	0.18	Immunoluminescence	Abbott ARCHITECT I1000	0.272
13	0.19	Immunoluminescence	Abbott ARCHITECT I1000	0.230
14	0.2	Immunoluminescence	Abbott ARCHITECT I1000	0.302
15	0.24	Immunoluminescence	Abbott ARCHITECT I1000	0.251
16	0.33	Immunoluminescence	Abbott ARCHITECT I1000	0.366
17	0.34	Immunoluminescence	Abbott ARCHITECT I1000	0.543
18	0.35	Immunoluminescence	Abbott ARCHITECT I1000	0.376
19	0.35	Immunoluminescence	Abbott ARCHITECT I1000	0.594
20	0.39	Immunoluminescence	Abbott ARCHITECT I1000	0.724
21	0.39	Immunoluminescence	Abbott ARCHITECT I1000	0.548
22	0.39	Immunoluminescence	Abbott ARCHITECT I1000	0.476
23	0.4	Immunoluminescence	Abbott ARCHITECT I1000	0.567
24	0.48	Immunoluminescence	Abbott ARCHITECT I1000	0.623
25	0.48	Immunoluminescence	Abbott ARCHITECT I1000	0.722
26	0.49	Immunoluminescence	Abbott ARCHITECT I1000	0.530
27	0.49	Immunoluminescence	Abbott ARCHITECT I1000	0.736
28	0.52	Immunoluminescence	Abbott ARCHITECT I1000	0.756
29	0.53	Immunoluminescence	Abbott ARCHITECT I1000	1.046
30	0.53	Immunoluminescence	Abbott ARCHITECT I1000	0.590
31	0.58	Immunoluminescence	Abbott ARCHITECT I1000	0.849
32	0.58	Immunoluminescence	Abbott ARCHITECT I1000	0.960
33	0.63	Immunoluminescence	Abbott ARCHITECT I1000	0.891
34	0.68	Immunoluminescence	Abbott ARCHITECT I1000	0.843
35	0.74	Immunoluminescence	Abbott ARCHITECT I1000	1.055
36	0.96	Immunoluminescence	Abbott ARCHITECT I1000	1.897
37	0.96	Immunoluminescence	Abbott ARCHITECT I1000	1.232
38	1.03	Immunoluminescence	Abbott ARCHITECT I1000	1.863
39	1.18	Immunoluminescence	Abbott ARCHITECT I1000	1.195
40	3.48	Immunoluminescence	Abbott ARCHITECT I1000	6.368
41	3.6	Immunoluminescence	Abbott ARCHITECT I1000	7.108
42	7.49	Immunoluminescence	Abbott ARCHITECT I1000	13.626
43	11.27	Immunoluminescence	Abbott ARCHITECT I1000	1.000

44	12.24	Immunoluminescence	Abbott ARCHITECT I1000	19.242
45	12.24	Immunoluminescence	Abbott ARCHITECT I1000	15.307
46	14.76	Immunoluminescence	Abbott ARCHITECT I1000	27.683
47	15.05	Immunoluminescence	Abbott ARCHITECT I1000	19.983
48	15.05	Immunoluminescence	Abbott ARCHITECT I1000	16.094
49	18.36	Immunoluminescence	Abbott ARCHITECT I1000	27.317
50	25.92	Immunoluminescence	Abbott ARCHITECT I1000	43.056
51	557.28	Immunoluminescence	Abbott ARCHITECT I1000	1056.865
52	557.28	Immunoluminescence	Abbott ARCHITECT I1000	697.514
53	583.2	Immunoluminescence	Abbott ARCHITECT I1000	1008.207
54	673.92	Immunoluminescence	Abbott ARCHITECT I1000	850.537
55	737.45	Immunoluminescence	Abbott ARCHITECT I1000	895.660
56	744.31	Immunoluminescence	Abbott ARCHITECT I1000	981.601
57	751.68	Immunoluminescence	Abbott ARCHITECT I1000	876.553
58	751.68	Immunoluminescence	Abbott ARCHITECT I1000	1371.536
59	777.6	Immunoluminescence	Abbott ARCHITECT I1000	1490.730
60	792.33	Immunoluminescence	Abbott ARCHITECT I1000	1560.479
61	803.52	Immunoluminescence	Abbott ARCHITECT I1000	1105.611
62	888.37	Immunoluminescence	Abbott ARCHITECT I1000	1233.796
63	972	Immunoluminescence	Abbott ARCHITECT I1000	1379.383
64	1016.75	Immunoluminescence	Abbott ARCHITECT I1000	1372.378
65	1016.75	Immunoluminescence	Abbott ARCHITECT I1000	1034.765

References

Chen, T.W., Rajaji, U., Chen, S.M., Lou, B.S., Al-Zaqri, N., Alsalme, A., Alharthi, F.A., Lee, S.Y., Chang, W.H., 2019. A sensitive electrochemical determination of chemotherapy agent using graphitic carbon nitride covered vanadium oxide nanocomposite; sonochemical approach. Ultrason. Sonochem. 58. https://doi.org/10.1016/j.ultsonch.2019.104664

Deng, Z., Tian, Q., Xu, Y., Lun, L., Sun, S., Yang, X., Liu, R., Zhou, Y., Li, H., Zhou, T., 2020. Rapid and sensitive detection of methotrexate using acetylene black electrode. Int. J. Electrochem. Sci. 15, 5058–5066. https://doi.org/10.20964/2020.06.84

Li, J., Chen, D., Zhang, T., Chen, G., 2021. Highly sensitive electrochemical determination of methotrexate based on a N-doped hollow nanocarbon sphere modified electrode. Anal. Methods 13, 117–123. https://doi.org/10.1039/d0ay01996h

Wang, Y., Xie, J., Tao, L., Tian, H., Wang, S., Ding, H., 2014. Simultaneous electrochemical determination of epirubicin and methotrexate in human blood using a disposable electrode modified with nano-Au/MWNTs-ZnO composites. Sensors Actuators, B Chem. 204, 360–367. https://doi.org/10.1016/j.snb.2014.07.099